Polymer Bulletin (2022) 79:1467–1484
https://doi.org/10.1007/s00289-021-03564-6

ORIGINAL PAPER

Novel polycarbonate membrane embedded with multi-walled carbon nanotube for water treatment: a comparative study between bovine serum albumin and humic acid removal

Homayun Khezraqa[1] · Habib Etemadi[1] · Hamidreza Qazvini[1] · Mehdi Salami-Kalajahi[2]

Received: 11 September 2020 / Revised: 21 December 2020 / Accepted: 22 January 2021 /
Published online: 6 February 2021

Abstract

Flat sheet polycarbonate/multi-walled carbon nanotube (PC/MWCNT) nanocomposite membranes with different nanoparticle contents were prepared by applying the phase inversion method. The characteristics of the prepared membranes were analyzed by field emission scanning electron microscopy (FE-SEM), atomic force microscopy (AFM), water contact angle, porosity, pure water flux (PWF), and mechanical properties. The performance of the membranes was evaluated in a submerged membrane system for two cycles and also for the filtration of humic acid (HA) and bovine serum albumin (BSA). The obtained results revealed that nanocomposites containing 0.1 wt% of MWCNTs showed better hydrophilicity, porosity, PWF, and mechanical properties. The FE-SEM images from surface indicated that the density and pore size of membrane increased from 0 to 0.1 wt% of MWCNTs. Moreover, according to AFM images, the PC/MWCNT-0.1 membrane showed a smoother surface than other samples. The antifouling performance of the membranes in a submerged membrane system revealed that the BSA solution flux for all membranes was lower than that of the HA solution due to the pore blocking of membranes occurring in the initial filtration of BSA. Apart from that addition of the 0.1 wt% of MWCNTs led to significant improvement in the fouling recovery ratio in the filtration of both HA and BSA because of the lower roughness and high hydrophilicity of the membrane surface. The rejection results revealed that the neat PC membrane had the highest value in the removal of HA and BSA with respect to other samples due to the formation of a thicker and denser cake layer on the membrane surface.

Keywords Polycarbonate membrane · MWCNTs · Phase inversion · Antifouling · Submerged membrane system

✉ Habib Etemadi
h_etemadi@ubonab.ac.ir

Extended author information available on the last page of the article

Introduction

Today, demand for clean water is increasing enormously in many areas across the world. However, activities in the domestic, agriculture, and industrial sectors among others release a large amount of pollutants into surface water [1]. Therefore, finding a way for treatment and removal of pollutants from contaminated water would be a major step toward solving much of the world's water problems. Among the existing technologies such as chemical oxidation, chlorination or ozonation, activated carbon adsorption, and coagulation, polymer membrane filtration has been widely used because of its flexibility, easy scale-up production, low cost, and low chemical consumption [2, 3]. However, it is well known that membrane fouling poses the biggest challenge to the membrane separation process, thereby resulting in low flux, recovery and rejection rate, and high energy costs [4, 5].

Using very low cost polymer for the fabrication of membrane can significantly reduce overall and operational costs in the membrane separation process, which would in turn give rise to cost-effective technology. In this case, polycarbonate (PC) polymer can be considered as a good candidate for membrane fabrication due to its unique physical and chemical properties such as excellent physical properties, good mechanical strength, high heat resistance, chemical resistances, and very low costs [6, 7]. However, hydrophilicity, porosity of PC as well as effective removal of pollutants still need to be improved. In other words, the wettability of PC membrane is not optimal, causing membrane fouling due to hydrophobic interactions between the foulant and the membrane surface.

A promising way to improving the antifouling properties of the polymer membrane is utilization of nanoparticles [8–10]. Addition of inorganic nanostructures into membrane matrix could increase the hydrophilicity of membranes and the fouling resistance [11]. In this regard, a few reports were focused on the preparation of PC nanocomposite membranes. Delavar et al. [6] used PC nanocomposite membrane containing hydrous manganese oxide (HMO) and alumina nanoparticles for the removal of Cd^{+2} and Cu^{+2}. They concluded that the PC nanocomposite containing 15 wt% loading of both nanoparticles showed the highest pure water flux and hydrophilicity. Meanwhile, PC/HMO nanocomposite membranes are obviously more efficient in heavy metal ions removal when compared to PC/alumina nanocomposite membrane.

Among nanoparticles, multi-wall carbon nanotubes (MWCNT) have been widely used in the preparation of polymer nanocomposite membranes for the removal of various contaminants from contaminated water [12] due to its large specific surface area [13], high adsorption capacity for organic matter [14], high stability and mechanical strength and relatively low price [15], as well as acting as extraordinary mass transport channels [16–18]. According to literature, several polymers such as polyethersulfone (PES) [12, 19–21], polysulfone (PSf) [22, 23], aromatic polyamide (PA) [24], polyvinylidene fluoride (PVDF) [25], cellulose acetate (CA) [26], polyvinyl chloride (PVC) [27, 28] have been used in the preparation of polymer/MWCNT nanocomposite membranes for water treatment.

Incorporating MWCNT in the PC polymer membranes for water treatment has not yet been reported in the literature. Therefore, this study investigates the effect of adding MWCNT on the morphology and performance of PC membranes in the water treatment. The membrane performance was characterized in a submerged membrane system for the removal of humic acid (HA) and bovine serum albumin (BSA) from contaminated surface water, and the obtained results were compared with each other. The membranes were fabricated via the non-solvent induced phase inversion separation (NIPS) method. Literature showed that few reports had been focused on the preparation of PC membrane via phase inversion process [29]. The fabricated nanocomposite membranes' properties and structure were characterized using water contact angle, field emission electron microscopy (FE-SEM) and pure water flux (PWF) analyses. The antifouling properties of nanocomposite membranes were investigated by HA and BSA solutions as foulants. BSA is one of the potential proteins largely focused upon due to its role in pharmaceutical and biotechnology research. Moreover, HA, a mixture of acids and a common pollutant present in most industrial wastewater sources, needs to be removed [30].

Experimental

Materials

Supplied from US Research Nanomaterials, multi-walled carbon nanotubes (MWCNTs) with an interior diameter of 5–10 nm and exterior diameter of 20–30 nm and a length of 1–5 µm (purity ≥ 95 wt%) were used as nanofillers. Polycarbonate (PC, grade: 0710) and polyethylene glycol (PEG) with molecular weight of 400 Da as pore former were purchased from Khuzestan Petrochemical Company (Iran) and Merck, respectively. *N*-methyl 2-pyrrolidone (NMP), purchased from Merck as well, was used as a solvent for the polymers. De-ionized (DI) water was used as non-solvent in the immersion precipitation non-solvent bath. Humic acid (HA) and bovine serum albumin (BSA, 66.5 KDa) powders, obtained from Sigma-Aldrich, USA, were used as the organic foulants.

Preparation of membranes

First, in order to improve the hydrophilicity of MWCNTs, thermal treatment was used according to Navarrete et al. study [31]. This method is a low cost and environmentally friendly process. For this purpose, MWCNTs were set inside a quartz tube and placed into an electric furnace at 270 °C temperature under atmospheric condition for 30 min.

In this study, the non-solvent induced phase separation (NIPS) method was used in the preparation of flat sheet neat PC and PC/MWCNT nanocomposite membranes. The polymer nanocomposite solutions for the membrane formation were prepared in NMP with 17 wt% PC and 4 wt% PEG with respect to the total volume of solution and 0.05, 0.1, and 0.2 wt% MWCNTs with respect to the polymer (PC

and PEG) constituents. For the preparation of the solution, MWCNTs were mixed with NMP and the resultant mixture was subjected to sonication (ultrasonic bath) for 2 h. Then, PC and PEG were added to the dispersion and the mixture was stirred for 24 h at room temperature to obtain a homogeneous solution. After that it was degassed to ensure a complete removal of air bubbles before membrane casting. The casting solution was cast onto a smooth glass plate to form a film of 150-μm thickness and subsequently it was immersed into water coagulation bath. Then, the membranes were stored in DI water bath for 24 h to complete the removal of residual solvent.

Membrane characterization and testing

The chemical structure of MWCNTs was studied by Fourier transform infrared spectroscopy (FTIR) with a FT-IR Shimadzu (IRAffinity-1S) spectrometer in the range of 400–4000 cm^{-1}. The surface and cross-sectional morphologies of the neat PC and PC/MWCNTs nanocomposite membranes were characterized using field emission scanning electron microscope (FESEM; MIRA3 FEG-SEM, Tescan) operating at 15 kV. Membrane samples were cut into an appropriate size and coated with a thin film of gold before being mounted on the sample holder.

The roughness of membrane surfaces was analyzed using atomic force microscopy (AFM, Nanosurf Mobile S microscope). The membrane surface was then scanned with a laser beam reflected by cantilever within a scanning area of 5 μm × 5 μm. The roughness and 3D micrograph of the membrane surfaces were reported.

The static water contact angle goniometer (PGX, Thwing-Albert Instrument Co., USA) was used to characterize the membrane surface hydrophilicity. The reported contact angles are the results of the average of five measurements at different points of a membrane sample. The mechanical strength, including the tensile stress and strain parameters of the prepared membranes, were performed by tensile testing machine (Santam STM-5, Iran). The membrane samples were cut into rectangular shape, and the loading velocity was set as 10 mm/min.

The overall porosity (ε) was determined by the gravimetric method. To correlate the results, measurements were repeated three times using Eq. (1) [32]:

$$\varepsilon(\%) = \frac{\frac{1}{d_w}(W_w - W_d)}{\frac{1}{d_w}(W_w - W_d) + \frac{W_d}{d_p}} \tag{1}$$

where W_w is the weight of wet membranes (g), W_d is the weight of dry membranes (g), d_w is the pure water density (0.998 g/cm^3), and d_p is the polymer density (1.2 g/cm^3).

The performances of the prepared neat PC and PC/MWCNTs nanocomposite membranes were evaluated through a submerged membrane system with 3 L volume capacity containing HA or BSA solutions with a concentration of 1 g/L to be treated as well as an effective membrane surface area of 14.7 cm^2. The filtration trans-membrane pressure (TMP) was maintained at 0.2 bar by the vacuum pump. The air flow was provided

at a rate of 4 L min^{-1} to produce scouring on the membrane surface as well as to keep the HA or BSA particles in suspension in the tank. Each membrane was initially pressurized at TMP of 0.8 bar for 30 min to get a steady permeate flow. Then, TMP was reduced to the operating level of 0.2 bar. The pure water flux (PWF) was calculated by the following Eq. (2):

$$\mathrm{PWF} = \frac{V}{A \cdot t} \tag{2}$$

where V is the volume of permeated water (L), A is the membrane area (m^2), and t is the permeation time (h).

To analyze the fouling resistance of prepared nanocomposite membranes, following PWF tests (J_0), the experiments were followed by HA or BSA solutions and the flux (J_1) was measured at the vacuum pressure of 0.2 bar for 2 h. After filtration of the solutions, the membrane was cleaned with distilled water and then submerged in pure water tank to measure PWF after fouling (J_2). This cycle was performed three times. The flux recovery ratio (FRR) was calculated as follows:

$$\mathrm{FRR}(\%) = \frac{J_2}{J_1} \times 100 \tag{3}$$

Reversible fouling ratio (RFR) and irreversible fouling ratio (IFR) were defined and calculated by the following equations:

$$\mathrm{RFR}(\%) = \frac{J_2 - J_1}{J_0} \times 100 \tag{4}$$

$$\mathrm{IFR}(\%) = \frac{J_0 - J_2}{J_0} \times 100 \tag{5}$$

The total fouling ratio (TFR) was also defined and calculated as follows:

$$\mathrm{TFR}(\%) = \frac{J_0 - J_1}{J_0} \times 100 \tag{6}$$

The rejection (R) was calculated using Eq. (7):

$$R(\%) = \left(\frac{C_f - C_p}{C_f}\right) \times 100 \tag{7}$$

where C_f and C_p represent concentrations of HA or BSA in feed and permeate, respectively.

Results and discussion

FTIR analysis

The spectra of pristine and modified MWCNTs are compared in Fig. 1. The free OH stretch peak.

was found in the modified MWCNTs at 3500–3600 cm^{-1}, indicating a hydrogen O–H bond [31]. The bands in the 1550–1750 cm^{-1} range can be assigned to C=O groups and the bands in the range 950–1300 cm^{-1} confirm the presence of C–O bonds [33].

Hydrophilicity, porosity, PWF and mechanical properties

The hydrophilicity of the neat PC and PC/MWCNT nanocomposite membranes was evaluated by measuring the water contact angle and the results are presented in Table 1. As shown in Table 1, the contact angle declined significantly with the addition of MWCNTs into the PC polymer matrix. The neat PC membrane showed the highest water contact angle of 77.5°. Any further addition of MWCNTs, obviously when the nanoparticles content reached 0.1 wt%, caused more.

reduction in the contact angle and subsequently higher hydrophilicity. For the PC/MWCNT-0.1 nanocomposite membrane, the water contact angle was reduced to 64.1°. However, when amount of MWCNT increased to 0.1 wt%, it did not result in remarkable further enhancement of hydrophilicity. This might be explained by the irregular positioning of MWCNTs in the PC membrane structure at over 0.1 wt% MWCNT content, which leads to aggregation and reduces the effective surface of MWCNTs [16, 34].

The porosity of the prepared membrane was calculated based on Eq. (1), and the obtained results are shown in Table 1. Addition of MWCNTs up to 0.1 wt% to PC matrix, porosity increased from 62.3 to 68%. Mixing hydrophilic MWCNTs with

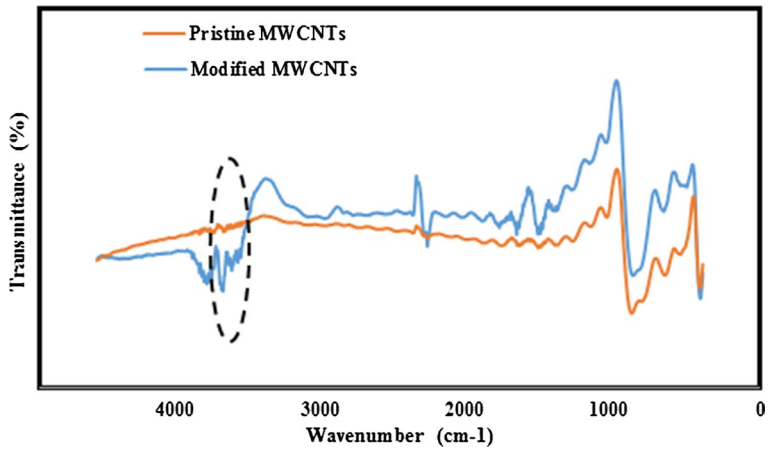

Fig. 1 FTIR spectra of pristine and modified MWCNTs

Table 1 water contact angle, porosity, PWF, and mechanical properties of prepared membranes

Membrane	Water contact angle (°)	Porosity (%)	PWF ($Lm^{-2}\ h^{-1}$)	Tensile strength (MPa)	Elongation at break (%)
Neat PC	77.5 (±2.4)	62.3 (±1.2)	22.6 (±4.2)	8.8 (±0.5)	15.1 (±2.3)
PC/MWCNT-0.05	75.6 (±3)	65.1 (±1.4)	30.7 (±3.6)	9.7 (±0.8)	17.2 (±2.8)
PC/MWCNT-0.1	64.1 (±2.2)	68 (±1.8)	45.8 (±4)	13.3 (±1.1)	21.3 (±3)
PC/MWCNT-0.2	63 (±2.5)	66.4 (±1.5)	39.5 (±3.2)	9.5 (±0.7)	16 (±3.2)

the matrix of PC polymer could enhance the volume fraction between the polymer chains, besides causing a fast exchange of solvents and non-solvents during the phase inversion process [35, 36]. Higher contents of MWCNTs do not yield any further increase in the porosity of nanocomposite membranes. This finding may contribute to particle agglomeration [37].

The effect of MWCNTs on the PWF of prepared membranes is shown in Table 1. All nanocomposite membranes show higher PWF with respect to neat PC membrane. According to Table 1, PWF for PC/MWCNT-0.1 nanocomposite membrane was 45.8 $Lm^{-2}\ h^{-1}$, which shows more than 100% increment in the PWF of neat PC membrane (22.6 $Lm^{-2}\ h^{-1}$). According to literature, hydrophilicity and porosity are two parameters affecting the PWF of membranes [38–40]. As shown in Table 1, the PC/MWCNT-0.1 nanocomposite membrane has the highest value in porosity and shows a low water contact angle.

Mechanical properties including tensile strength and elongation at break for all prepared membranes are listed in Table 1. Generally, during normal membrane operation, membrane unusable when stresses that cause irreversible deformation of the membrane material [41]. According to the obtained results, the tensile strength of neat PC membrane is about 8.8 MPa. In comparison with the neat PC membrane, when MWCNTs contents increase up to 0.1 wt%, the tensile strength and elongation at break of nanocomposite membranes increase about 51.1% and 41%, respectively. When MWCNTs contents increase up to 0.2 wt%, a decline in the tensile strength and elongation at break is observed that may be due to the agglomeration of nanoparticles in higher concentration.

Morphology of prepared membranes

In order to evaluate the morphology studies of neat PC and nanocomposite membranes, FE-SEM images were taken from top surface and cross-sectional of membranes. The FE-SEM images of the top surface of neat PC and PC/MWCNT-0.1 nanocomposite membranes are presented in Fig. 2. According to this figure, both density and pore size of the membranes increased from 0 to 0.1 wt% of the MWCNTs. In this case, pore size distribution for both membranes was performed by the Digimizer image analysis software and the obtained results are depicted in Fig. 3. It is clear that in the PC/MWCNT-0.1 nanocomposite membrane, the number of large pores (> 12 nm) was increased. This change in morphology is explained by the fact of an increase in the mass transfer rate between solvent and non-solvent by adding the functionalized MWCNTs as hydrophilic materials [25, 42].

Figure 4 depicts the FE-SEM images of cross-sectional of membranes. As observed in Fig. 4, the cross section of both membranes has an asymmetric structure with three layers: the top layer with a thin dense selective barrier, the sub-layer with a finger-like structure and the bottom layer with much thicker porous substructure and macrovoids. This morphology was observed in the PES/MWCNT nanocomposite nanofiltration membranes [43]. By comparing Fig. 4a and b, it is observed that by addition of 0.1 wt% of MWCNTs to the PC matrix, the size of finger-like and macrovoid structures increased. The presence of

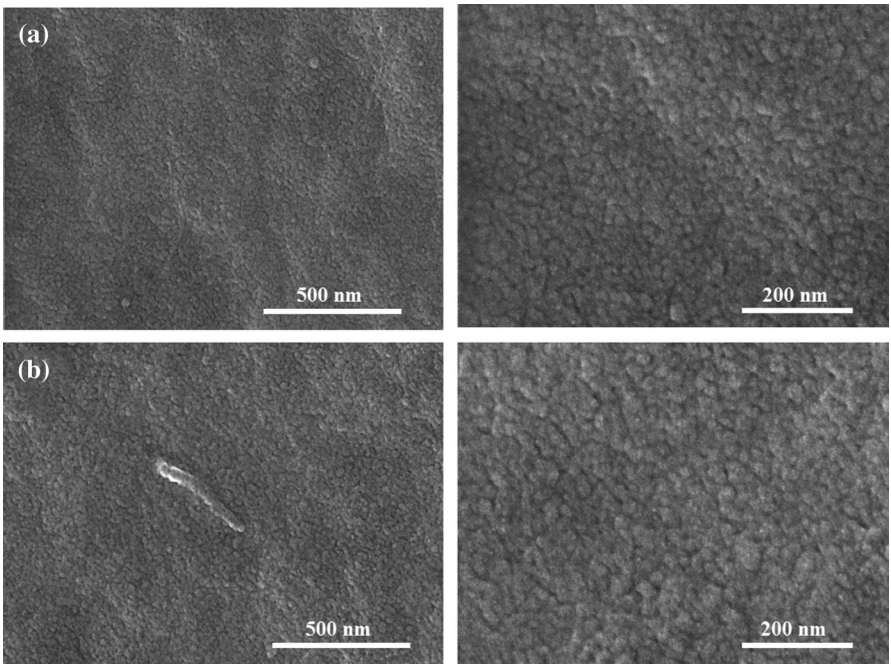

Fig. 2 FE-SEM images of the top surface of (**a**) neat PC and (**b**) PC/MWCNT-0.1 nanocomposite membranes

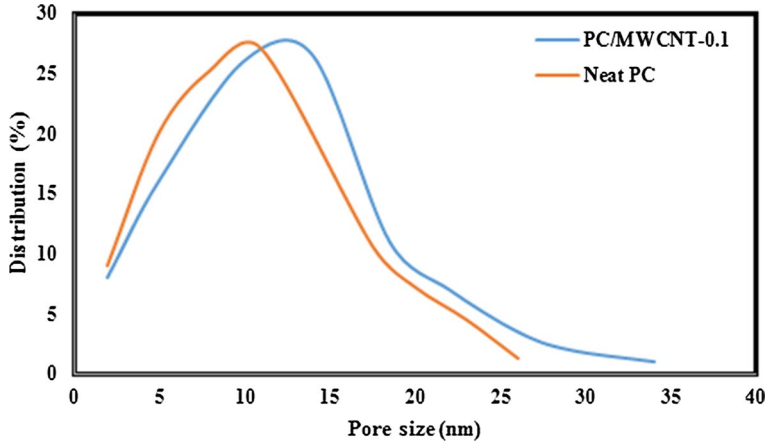

Fig. 3 Pore size distribution of the neat PC and PC/MWCNT-0.1 nanocomposite membranes

hydrophilic MWCNTs in the structure of nanocomposite membrane during phase inversion process accelerates the rate of solvent (NMP) and non-solvent (water) exchange, thereby resulting in higher porosity and bigger macrovoids [44, 45].

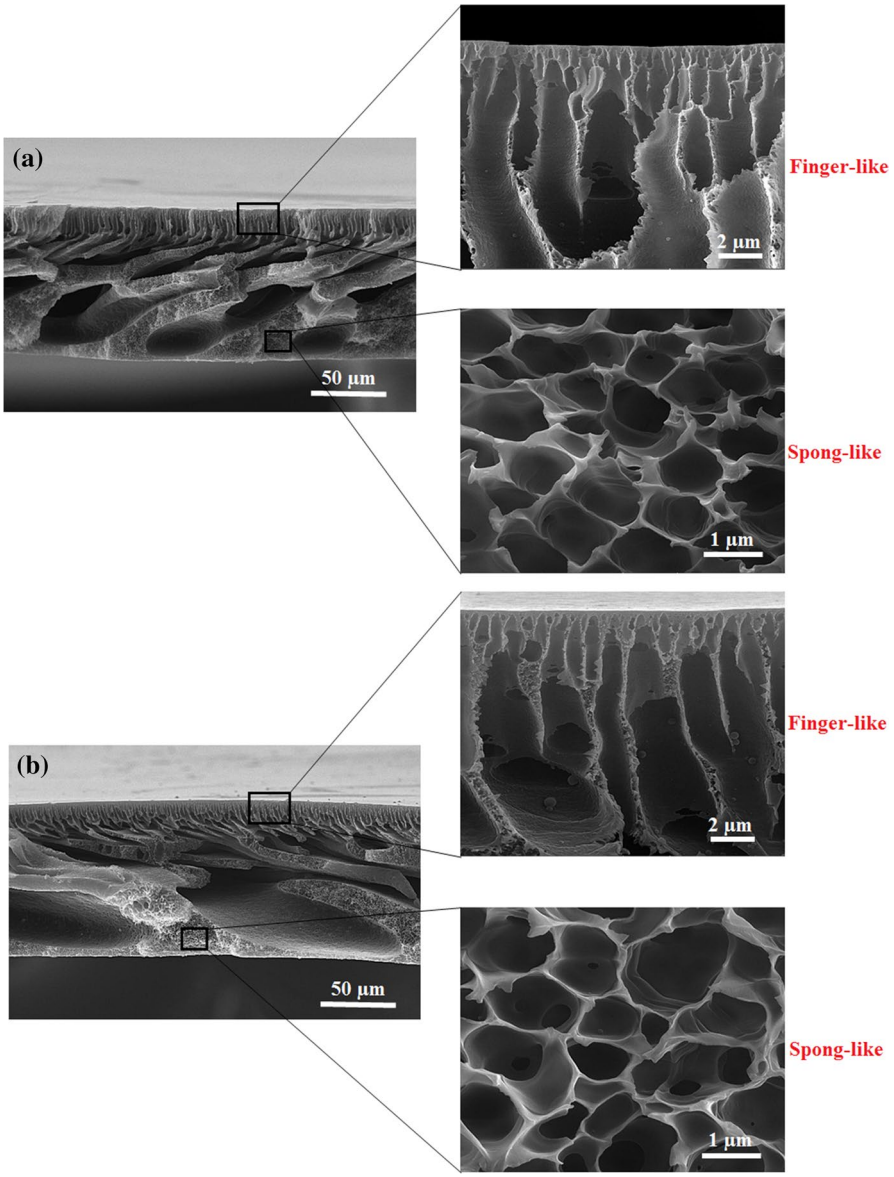

Fig. 4 FE-SEM images of the cross section of (**a**) neat PC and (**b**) PC/MWCNT-0.1 nanocomposite membranes

Figure 5 shows the three-dimensional AFM images of membranes. As can be seen, the surface topology of the prepared nanocomposite membrane is affected by addition of MWCNTs nanoparticles to the casting solution. The surface roughness parameters of both membranes are presented in Table 2. According to Table 2, PC/MWCNT-0.1 nanocomposite membrane has a lower value in the roughness

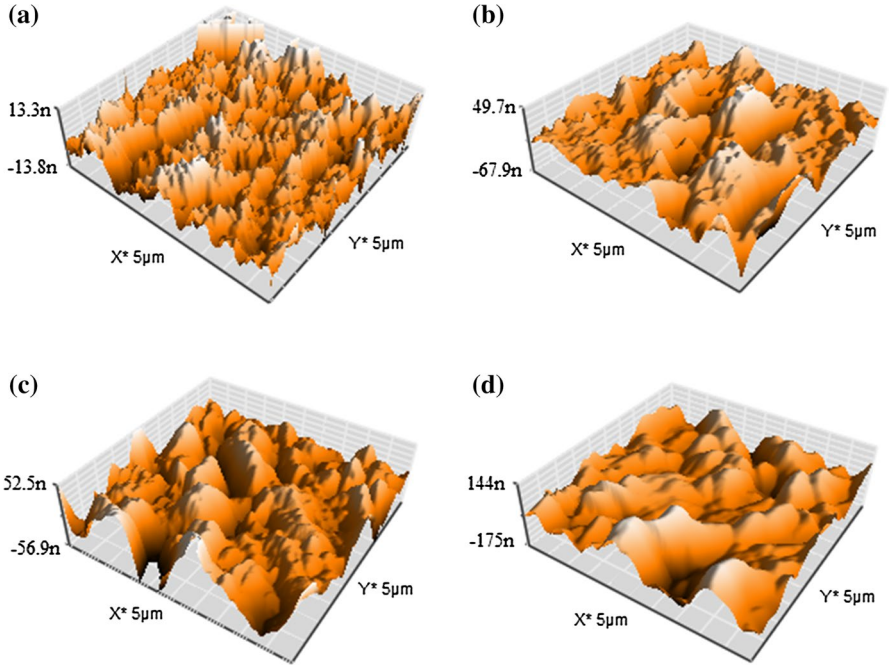

Fig. 5 Surface AFM images of the prepared membranes with different concentrations of MWCNTs: **a** neat PC, **b** 0.05 wt%, **c** 0.1 wt%, and **d** 0.2 wt%

Table 2 Surface roughness parameters of the prepared membranes

Membranes	R_a (nm)	R_q (nm)	R_y (nm)
Neat PC	25.8	31.6	130.1
PC/MWCNT-0.05	15.6	20.4	90.7
PC/MWCNT-0.1	10.8	13	63.4
PC/MWCNT-0.2	22.1	27.2	120.5

parameters as compared to other samples. However, due to an increase in the agglomeration of carbon nanotubes, the roughness of the membrane surface was increased by mixing the high concentration of MWCNTs (0.2 wt%) [21]. According to literature, the membrane fouling phenomena tended to be more significantly related to roughness owing to contaminants accumulating in the valleys of rough membrane surfaces [46, 47].

Antifouling performance of membranes in the filtration of HA and BSA

The antifouling performance of the neat PC and PC/MWCNT nanocomposite membranes was characterized by measuring water flux recovery after fouling by HA and BSA solutions. The results are shown in Fig. 6. The objective is to demonstrate the

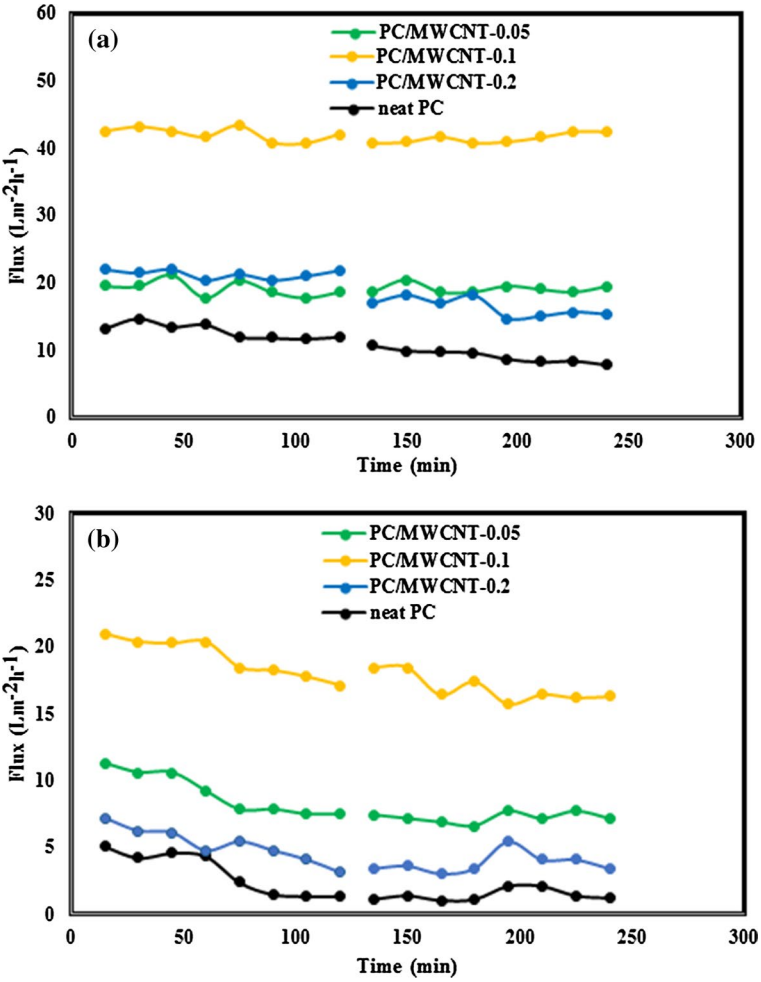

Fig. 6 Time dependence behavior of flux of the prepared membranes in the filtration of (**a**) HA and (**b**) BSA solutions

importance of membrane cleaning and the performance decline in 2 cycles. During the two filtration cycles (120 min each, one physical cleaning in between) with different foulant, i.e., HA and BSA, the flux-time behavior of membrane was investigated in order to assess the membrane performance. As shown in Fig. 6a and for HA filtration, no significant decline in the flux versus time trend was observed in all the membranes in each filtration cycle. Moreover, among all membranes, PC/MWCNT-0.1 showed a higher flux with respect to other samples. These values are 41 Lm^{-2} h^{-1} for both cycles of filtration. It is clear that MWCNTs improved the flux of neat PC membranes. It means that the filtration performance of the prepared nanocomposite membranes was enhanced when they were exposed to the HA solution.

Figure 6b shows filtration of the BSA solution for all membranes in the two cycles of filtration. It is observed that in the first cycle, the trend of flux versus time declines, while in the second cycle of filtration, this trend is constant. Although all membranes showed similar trends of BSA flux decline in the first cycle, a higher BSA flux was seen after increasing MWCNTs concentration up to 0.1 wt% (17 $Lm^{-2} h^{-1}$).

Comparing the flux versus time trend of the membranes in HA and BSA filtration reveal that all membranes show a higher flux in the filtration of HA when compared to the BSA filtration. Therefore, membrane fouling initially occurs inside the pore in the case of the BSA filtration, while HA is deposited on the membrane surface even in the initial stage of fouling [48].

To investigate the antifouling performance of membranes in the filtration of BSA and HA, the fouling parameters were calculated for both cycles and the obtained results are shown in Table 3. In the case of HA and for the first cycle, the neat PC membrane had a high IFR (15.6%), due to lower hydrophilicity [49]. Among the nanocomposite membranes, the PC/MWCNT-0.2 membrane represented the highest irreversible fouling, which can be attributed to higher roughness as shown in Table 2. Meanwhile, the PC/MWCNT-0.1 membrane had the highest FRR value of 95.2% and the lowest IFR value of 4.8%. As shown in Table 3, in the second cycles, IFR and FRR for all membranes decreased and increased slightly, respectively. A similar trend was observed elsewhere [50]. Therefore, a comparison between the cycles indicated that PC/MWCNT membranes exhibit a promising performance since no significant flux drop was observed from cycle to cycle in the HA filtration.

In the case of BSA filtration, the fouling parameters significantly increased when compared to HA filtration. As noted, it may be due to the pore blocking of

Table 3 Fouling parameters of membranes for filtration of HA and BSA

Sample	Foulant type	State	RFR (%)	IFR (%)	TFR (%)	FRR (%)
Neat PC	HA	Cycle 1	30.9	15.6	46.5	84.3
		Cycle 2	38.4	14.2	52.6	85.8
	BSA	Cycle 1	71.2	18.6	89.8	81.7
		Cycle 2	71.2	17.9	89.1	82.3
PC/MWCNT-0.05	HA	Cycle 1	30.6	7.5	38.1	92.6
		Cycle 2	26.4	6.9	33.3	93.5
	BSA	Cycle 1	62.8	11.7	74.5	88.4
		Cycle 2	63	11	74	89
PC/MWCNT-0.1	HA	Cycle 1	5.7	4.8	10.5	95.2
		Cycle 2	4.6	3.7	8.3	96.4
	BSA	Cycle 1	50.2	9.4	59.6	90.7
		Cycle 2	50	8.7	58.7	91.3
PC/MWCNT-0.2	HA	Cycle 1	37.7	9.1	46.8	91
		Cycle 2	48.7	8	56.7	91.9
	BSA	Cycle 1	72.4	14.9	87.3	85.1
		Cycle 2	72.3	14.3	86.6	85.8

membranes occurring in the initial filtration of BSA as well as the presence of wonderful interaction between BSA molecules and the membrane surface. However, the PC/MWCNT-0.1 nanocomposite membrane shows better antifouling performance with respect to other samples in the BSA filtration. According to literature, the membrane fouling phenomena tended to be more significantly related to roughness owing to contaminants accumulating in the valleys of rough membrane surfaces [47]. As indicated in Table 2, the PC/MWCNT-0.1 nanocomposite membrane shows smoother surface when compared to other samples.

The rejection of the HA and BSA solutions for the neat PC and PC/MWCNT nanocomposite membranes is shown in Fig. 7. The results show that the neat PC membrane exhibited high protein rejection performance compared to other membranes. According to literature, foulant removal in the permeates was due to the simultaneous impact of

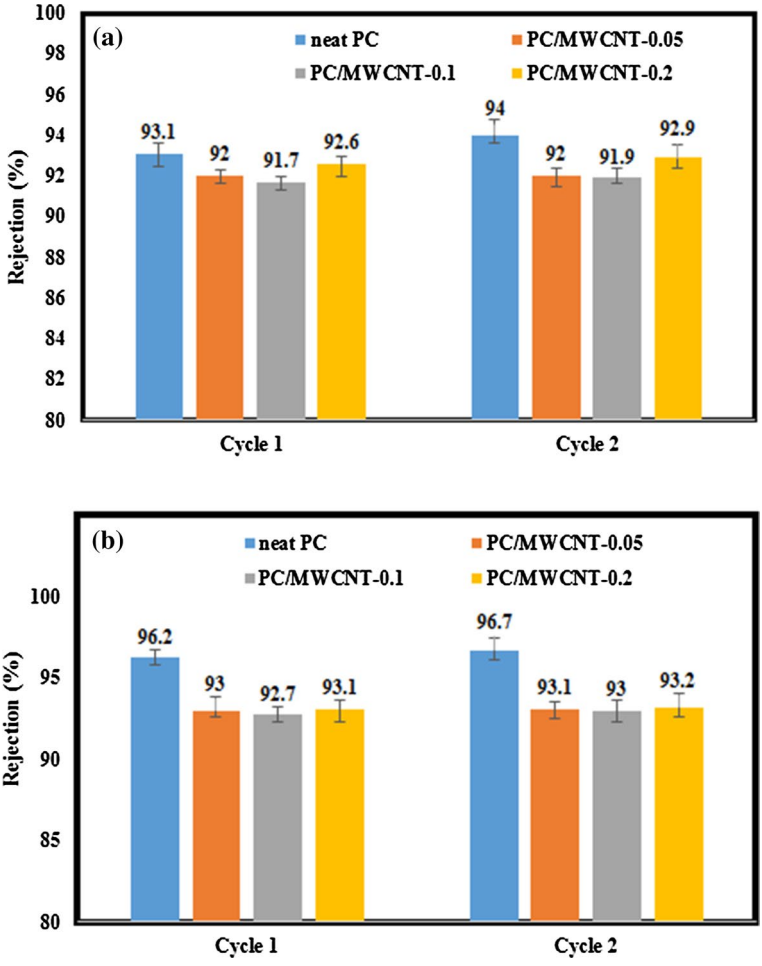

Fig. 7 Rejection performance of fabricated membranes in the filtration of (**a**) HA and (**b**) BSA solutions

membrane filtration and film formation on the membrane surfaces [51, 52]. The membrane fouling was mostly attributed to the pore blocking as well as to the formation of a cake layer. Since the cake layer formed on the neat PC membrane surface was more dense than the nanocomposite membranes, it acts as a secondary membrane that filters and prevents the penetration of foulants [53].

The rejection of BSA in Fig. 7b was higher than that of HA (Fig. 7a). This may be due to the pore blocking of membranes in the initial performance of the BSA filtration. Figure 7 indicated that there is no significant improvement in the HA and BSA rejection for the first and second cycles. These results revealed that efficiency occurs in the early stages and might not have a great impact on the long term performance of the membranes.

Conclusion

In this study, novel PC/MWCNT nanocomposite membranes were fabricated successfully using the NIPS method. The FTIR spectra confirmed that the hydroxyl group was formed on the MWCNTs surface by applying the thermal treatment method. The neat PC and nanocomposite membranes were evaluated in a submerged membrane system for the filtration of HA and BSA, and the obtained results were compared in the two cycles of filtration. The results showed that the water contact angle of PC/MWCNT nanocomposite membranes decreased, indicating improvement in the hydrophilicity of the membrane surface. The porosity and PWF values of the fabricated membranes demonstrated that incorporation of 0.1 wt% of MWCNTs to the polymer dope solution showed higher values when compared to other samples. The FE-SEM images indicated that both density and pore size of the membranes increased from 0 to 0.1 wt% of the MWCNTs. Furthermore, by adding 0.1 wt% of MWCNTs to PC matrix, the size of finger-like and macrovoid structures increased.

The antifouling performance of neat PC and PC/MWCNT nanocomposite membranes showed that all nanocomposite membranes had a higher flux in the filtration of HA and BSA solutions with respect to neat PC membrane. However, the flux of BSA solution for all membranes was lower than for the HA solution, which was due to the pore blocking of membranes occurring in the initial filtration of BSA. Meanwhile, the PC/MWCNT-0.1 membrane had the highest FRR value of 95.2% and the lowest IFR value of 4.8% in the first cycle of HA filtration. In conclusion, although the membranes showed a higher BSA rejection than HA rejection, no significant improvement was observed from cycle to cycle, and in this case the neat PC membrane had the highest value of HA and BSA rejection with respect to other samples, which was due to the thicker and denser cake layer on the membrane surface.

References

1. Ali S, Rehman SAU, Luan HY, Farid MU, Huang H (2019) Challenges and opportunities in functional carbon nanotubes for membrane-based water treatment and desalination. Sci Total Environ 646:1126–1139

2. Irani E, Amoli-Diva M (2020) Hybrid adsorption–photocatalysis properties of quaternary magneto-plasmonic ZnO/MWCNTs nanocomposite for applying synergistic photocatalytic removal and membrane filtration in industrial wastewater treatment. J Photoch Photobio A 391:112359
3. Ho K, Teow Y, Mohammad A, Ang W, Lee P (2018) Development of graphene oxide (GO)/multi-walled carbon nanotubes (MWCNTs) nanocomposite conductive membranes for electrically enhanced fouling mitigation. J Membr Sci 552:189–201
4. Van der Bruggen B, Braeken L, Vandecasteele C (2002) Evaluation of parameters describing flux decline in nanofiltration of aqueous solutions containing organic compounds. Desalination 147:281–288
5. Etemadi H, Qazvini H (2020) Investigation of alumina nanoparticles role on the critical flux and performance of polyvinyl chloride membrane in a submerged membrane system for the removal of humic acid. Polym Bull 2020:1–18
6. Delavar M, Bakeri G, Hosseini M (2017) Fabrication of polycarbonate mixed matrix membranes containing hydrous manganese oxide and alumina nanoparticles for heavy metal decontamination: characterization and comparative study. Chem Eng Res Des 120:240–253
7. Idris A, Man Z, Maulud AS (2017) Polycarbonate/silica nanocomposite membranes: fabrication, characterization, and performance evaluation. J Appl Polym Sci 134:45310
8. Ebert K, Fritsch D, Koll J, Tjahjawiguna C (2004) Influence of inorganic fillers on the compaction behaviour of porous polymer based membranes. J Membr Sci 233:71–78
9. Yan L, Hong S, Li ML, Li YS (2009) Application of the Al2O3–PVDF nanocomposite tubular ultrafiltration (UF) membrane for oily wastewater treatment and its antifouling research. Sep Purif Technol 66:347–352
10. Etemadi H, Yegani R, Seyfollahi M (2017) The effect of amino functionalized and polyethylene glycol grafted nanodiamond on anti-biofouling properties of cellulose acetate membrane in membrane bioreactor systems. Sep Purif Technol 177:350–362
11. Vatanpour V, Yekavalangi ME, Safarpour M (2016) Preparation and characterization of nanocomposite PVDF ultrafiltration membrane embedded with nanoporous SAPO-34 to improve permeability and antifouling performance. Sep Purif Technol 163:300–309
12. Rahimi Z, Zinatizadeh A, Zinadini S (2015) Preparation of high antibiofouling amino functionalized MWCNTs/PES nanocomposite ultrafiltration membrane for application in membrane bioreactor. J Ind Eng Chem 29:366–374
13. Sears K, Dumée L, Schütz J, She M, Huynh C, Hawkins S, Duke M, Gray S (2010) Recent developments in carbon nanotube membranes for water purification and gas separation. Materials 3:127–149
14. Lu C, Su F (2007) Adsorption of natural organic matter by carbon nanotubes. Sep Purif Technol 58:113–121
15. Xu J, Cao Z, Zhang Y, Yuan Z, Lou Z, Xu X, Wang X (2018) A review of functionalized carbon nanotubes and graphene for heavy metal adsorption from water: preparation, application, and mechanism. Chemosphere 195:351–364
16. Celik E, Park H, Choi H, Choi H (2011) Carbon nanotube blended polyethersulfone membranes for fouling control in water treatment. Water Res 45:274–282
17. Dumée LF, Sears K, Schütz J, Finn N, Huynh C, Hawkins S, Duke M, Gray S (2010) Characterization and evaluation of carbon nanotube Bucky-Paper membranes for direct contact membrane distillation. J Membr Sci 351:36–43
18. Majeed S, Fierro D, Buhr K, Wind J, Du B, Boschetti-de-Fierro A, Abetz V (2012) Multi-walled carbon nanotubes (MWCNTs) mixed polyacrylonitrile (PAN) ultrafiltration membranes. J Membr Sci 403:101–109
19. Saranya R, Arthanareeswaran G, Dionysiou DD (2014) Treatment of paper mill effluent using polyethersulfone/functionalised multiwalled carbon nanotubes based nanocomposite membranes. Chem Eng J 236:369–377
20. Sengur R, de Lannoy CF, Turken T, Wiesner M, Koyuncu I (2015) Fabrication and characterization of hydroxylated and carboxylated multiwalled carbon nanotube/polyethersulfone (PES) nanocomposite hollow fiber membranes. Desalination 359:123–140
21. Vatanpour V, Madaeni SS, Moradian R, Zinadini S, Astinchap B (2011) Fabrication and characterization of novel antifouling nanofiltration membrane prepared from oxidized multiwalled carbon nanotube/polyethersulfone nanocomposite. J Membr Sci 375:284–294
22. Shah P, Murthy C (2013) Studies on the porosity control of MWCNT/polysulfone composite membrane and its effect on metal removal. J Membr Sci 437:90–98

23. de Lannoy CF, Soyer E, Wiesner MR (2013) Optimizing carbon nanotube-reinforced polysulfone ultrafiltration membranes through carboxylic acid functionalization. J Membr Sci 447:395–402
24. Shawky HA, Chae SR, Lin S, Wiesner MR (2011) Synthesis and characterization of a carbon nanotube/polymer nanocomposite membrane for water treatment. Desalination 272:46–50
25. Vatanpour V, Ghadimi A, Karimi A, Khataee A, Yekavalangi ME (2018) Antifouling polyvinylidene fluoride ultrafiltration membrane fabricated from embedding polypyrrole coated multiwalled carbon nanotubes. Mater Sci Eng C 89:41–51
26. El Badawi N, Ramadan AR, Esawi AM, El-Morsi M (2014) Novel carbon nanotube–cellulose acetate nanocomposite membranes for water filtration applications. Desalination 344:79–85
27. Zendehnam A, Rabieyan M, Hosseini SM, Mokhtari S (2015) Novel nanocomposite heterogeneous cation exchange membrane prepared by MWCNTs-co-silver nanolayer composite nanoparticles: physico/chemical characterization and investigation of concentration effect. Korean J Chem Eng 32:501–510
28. Jalal Sadiq A, Shabeeb KM, Khalil BI, Alsalhy QF (2020) Effect of embedding MWCNT-g-GO with PVC on the performance of PVC membranes for oily wastewater treatment. Chem Eng Commun 207:733–750
29. Etemadi H, Amirjangi A, Ghasemian N, Shokri E (2020) Synthesis and characterization of polycarbonate/TiO_2 ultrafiltration membranes: critical flux determination. Chem Eng Technol 43:2247–2258
30. Saraswathi MSA, Rana D, Melbiah JB, Mohan D, Nagendran A (2018) Effective removal of bovine serum albumin and humic acid contaminants using poly (amide imide) nanocomposite ultrafiltration membranes tailored with GO and MoS_2 nanosheets. Mater Chem Phys 216:170–176
31. Contreras-Navarrete J, Granados-Martínez F, Domratcheva-Lvova L, Flores-Ramírez N, Cisneros-Magaña M, García-González L, Zamora-Peredo L, Mondragón-Sánchez M (2015) MWCNTs oxidation by thermal treatment with air conditions. Superficies y vacío 28:111–114
32. Moslehyani A, Ismail A, Othman M, Matsuura T (2015) Design and performance study of hybrid photocatalytic reactor-PVDF/MWCNT nanocomposite membrane system for treatment of petroleum refinery wastewater. Desalination 363:99–111
33. Gómez S, Rendtorff NM, Aglietti EF, Sakka Y, Suárez G (2016) Surface modification of multiwall carbon nanotubes by sulfonitric treatment. Appl Surf Sci 379:264–269
34. Qiu S, Wu L, Pan X, Zhang L, Chen H, Gao C (2009) Preparation and properties of functionalized carbon nanotube/PSF blend ultrafiltration membranes. J Membr Sci 342:165–172
35. Zhang G, Lu S, Zhang L, Meng Q, Shen C, Zhang J (2013) Novel polysulfone hybrid ultrafiltration membrane prepared with TiO_2-g-HEMA and its antifouling characteristics. J Membr Sci 436:163–173
36. Hudaib B, Gomes V, Shi J, Zhou C, Liu Z (2018) Poly (vinylidene fluoride)/polyaniline/MWCNT nanocomposite ultrafiltration membrane for natural organic matter removal. Sep Purif Technol 190:143–155
37. Etemadi H, Yegani R, Babaeipour V (2017) Performance evaluation and antifouling analyses of cellulose acetate/nanodiamond nanocomposite membranes in water treatment. J Appl Polym Sci 134:44873
38. Behboudi A, Jafarzadeh Y, Yegani R (2016) Preparation and characterization of TiO_2 embedded PVC ultrafiltration membranes. Chem Eng Res Des 114:96–107
39. Le-Clech P, Chen V, Fane TA (2006) Fouling in membrane bioreactors used in wastewater treatment. J Membr Sci 284:17–53
40. Vatanpour V, Esmaeili M, Farahani MHDA (2014) Fouling reduction and retention increment of polyethersulfone nanofiltration membranes embedded by amine-functionalized multi-walled carbon nanotubes. J Membr Sci 466:70–81
41. Childress AE, Le-Clech P, Daugherty JL, Chen C, Leslie GL (2005) Mechanical analysis of hollow fiber membrane integrity in water reuse applications. Desalination 180:5–14
42. Chan KH, Wong ET, Khan MI, Idris A, Yusof NM (2014) Fabrication of polyvinylidene difluoride nano-hybrid dialysis membranes using functionalized multiwall carbon nanotube for polyethylene glycol (hydrophilic additive) retention. J Ind Eng Chem 20:3744–3753
43. Peydayesh M, Mohammadi T, Bakhtiari O (2018) Effective treatment of dye wastewater via positively charged TETA-MWCNT/PES hybrid nanofiltration membranes. Sep Purif Technol 194:488–502

44. Vatanpour V, Madaeni SS, Moradian R, Zinadini S, Astinchap B (2012) Novel antibifouling nanofiltration polyethersulfone membrane fabricated from embedding TiO2 coated multiwalled carbon nanotubes. Sep Purif Technol 90:69–82
45. Etemadi H, Yegani R, Babaeipour V (2016) Study on the reinforcing effect of nanodiamond particles on the mechanical, thermal and antibacterial properties of cellulose acetate membranes. Diam Relat Mater 69:166–176
46. Hong J, He Y (2014) Polyvinylidene fluoride ultrafiltration membrane blended with nano-ZnO particle for photo-catalysis self-cleaning. Desalination 332:67–75
47. Yan L, Li YS, Xiang CB, Xianda S (2006) Effect of nano-sized Al_2O_3-particle addition on PVDF ultrafiltration membrane performance. J Membr Sci 276:162–167
48. Watabe T, Matsuyama K, Takahashi T, Matsuyama H (2016) The effect of microbubbles on membrane fouling caused by different foulants. Desalin Water Treat 57:9558–9568
49. Huisman IH, Prádanos P, Hernández A (2000) The effect of protein–protein and protein–membrane interactions on membrane fouling in ultrafiltration. J Membr Sci 179:79–90
50. Ghiasi S, Behboudi A, Mohammadi T, Ulbricht M (2020) High-performance positively charged hollow fiber nanofiltration membranes fabricated via green approach towards polyethyleneimine layer assembly. Sep Purif Technol 251:117313
51. Etemadi H, Yegani R, Seyfollahi M, Babaeipour V (2017) Preparation and performance evaluation of cellulose acetate/nanodiamond nanocomposite membrane in the treatment of pharmaceutical wastewater by membrane bioreactor. Desalin Water Treat 76:98–111
52. Amini M, Etemadi H, Akbarzadeh A, Yegani R (2017) Preparation and performance evaluation of high-density polyethylene/silica nanocomposite membranes in membrane bioreactor system. Biochem Eng J 127:196–205
53. Wang C, Chen WN, Hu QY, Ji M, Gao X (2015) Dynamic fouling behavior and cake layer structure changes in nonwoven membrane bioreactor for bath wastewater treatment. Chem Eng J 264:462–469

Authors and Affiliations

Homayun Khezraqa[1] · Habib Etemadi[1] · Hamidreza Qazvini[1] · Mehdi Salami-Kalajahi[2]

[1] Department of Polymer Science and Engineering, University of Bonab, Bonab, Iran

[2] Department of Polymer Engineering, Sahand University of Technology, Tabriz, Iran